ACSNANO

www.acsnano.org

ARTICLE

Self-Powered Wireless Smart Sensor Node Enabled by an Ultrastable, Highly Efficient, and Superhydrophobic-Surface-Based Triboelectric Nanogenerator

Kun Zhao,[†] Zhong Lin Wang,[†,‡] and Ya Yang*[,†]

[†]Beijing Institute of Nanoenergy and Nanosystems, Chinese Academy of Sciences; National Center for Nanoscience and Technology (NCNST), Beijing 100083, P. R. China

[‡]School of Materials Science and Engineering, Georgia Institute of Technology, Atlanta, Georgia 30332-0245, United States

Supporting Information

ABSTRACT: **Wireless sensor networks will be responsible for a majority of the fast growth in intelligent systems in the next decade. However, most of the wireless smart sensor nodes require an external power source such as a Li-ion battery, where the labor cost and environmental waste issues of replacing batteries have largely limited the practical applications. Instead of using a Li-ion battery, we report an ultrastable, highly efficient, and superhydrophobic-surface-based triboelectric nanogenerator (TENG) to scavenge wind energy for sustainably powering a wireless smart temperature sensor node. There is no decrease in the output voltage and current of the TENG after continuous working for about 14 h at a wind speed of 12 m/s. Through a power management circuit, the TENG can deliver a constant output voltage of 3.3 V and a pulsed output current of about 100 mA to achieve highly efficient energy storage in a capacitor. A wireless smart temperature sensor node can be sustainably powered by the TENG for sending the real-time temperature data to an iPhone under a working distance of 26 m, demonstrating the feasibility of the self-powered wireless smart sensor networks.**

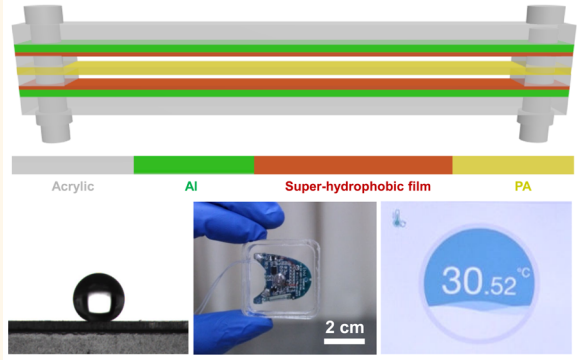

KEYWORDS: *triboelectric nanogenerator, wind energy, superhydrophobic, sensor, self-powered*

Due to the fast development of internet of things, wireless smart sensor networks/nodes have attracted increasing attention in the past decade for realizing the environmental detection, data analysis, and information monitoring.[1−3] An external power source such as a Li-ion battery is needed for powering these wireless sensor nodes, where these Li-ion batteries require periodic replacement due to their limited capacity and lifetime.[4−6] The main issue for preventing the extensive applications of the Li-ion batteries in wireless smart sensor networks is the periodic maintenance of the million wireless smart sensor nodes, which can result in a huge cost and expense. An ideal solution is to use an energy-scavenging device instead of the Li-ion battery to scavenge energy from the environment for sustainably powering individual sensor nodes, where the energy-scavenging devices are maintenance-free. Triboelectric nanogenerators (TENGs) have been extensively utilized to scavenge the ambient mechanical energy such as the vibrations, contact/separation motions, sliding motions, and rotation motions.[7−14] By using the wind-induced vibrations of an organic triboelectric film, the TENGs can scavenge wind energy in the natural environment.[15−17] However, the relatively low output performance of the wind energy harvesters cannot meet the needs of the large electric energy for most of the wireless sensor nodes. Moreover, these energy harvesters need to have good stability and to work under different weather conditions such as rain or lack of sunlight. To address these issues, it is necessary to develop an ultrastable, waterproof, and highly efficient TENG to scavenge wind energy for sustainably powering the wireless smart sensor nodes.

Here, we report an ultrastable, highly efficient, and superhydrophobic-surface-based TENG, which can be used to scavenge wind energy from all directions for sustainably powering a wireless smart temperature sensor node. The

Received: August 29, 2016
Accepted: September 6, 2016
Published: September 6, 2016

DOI: 10.1021/acsnano.6b05815
ACS Nano 2016, 10, 9044−9052

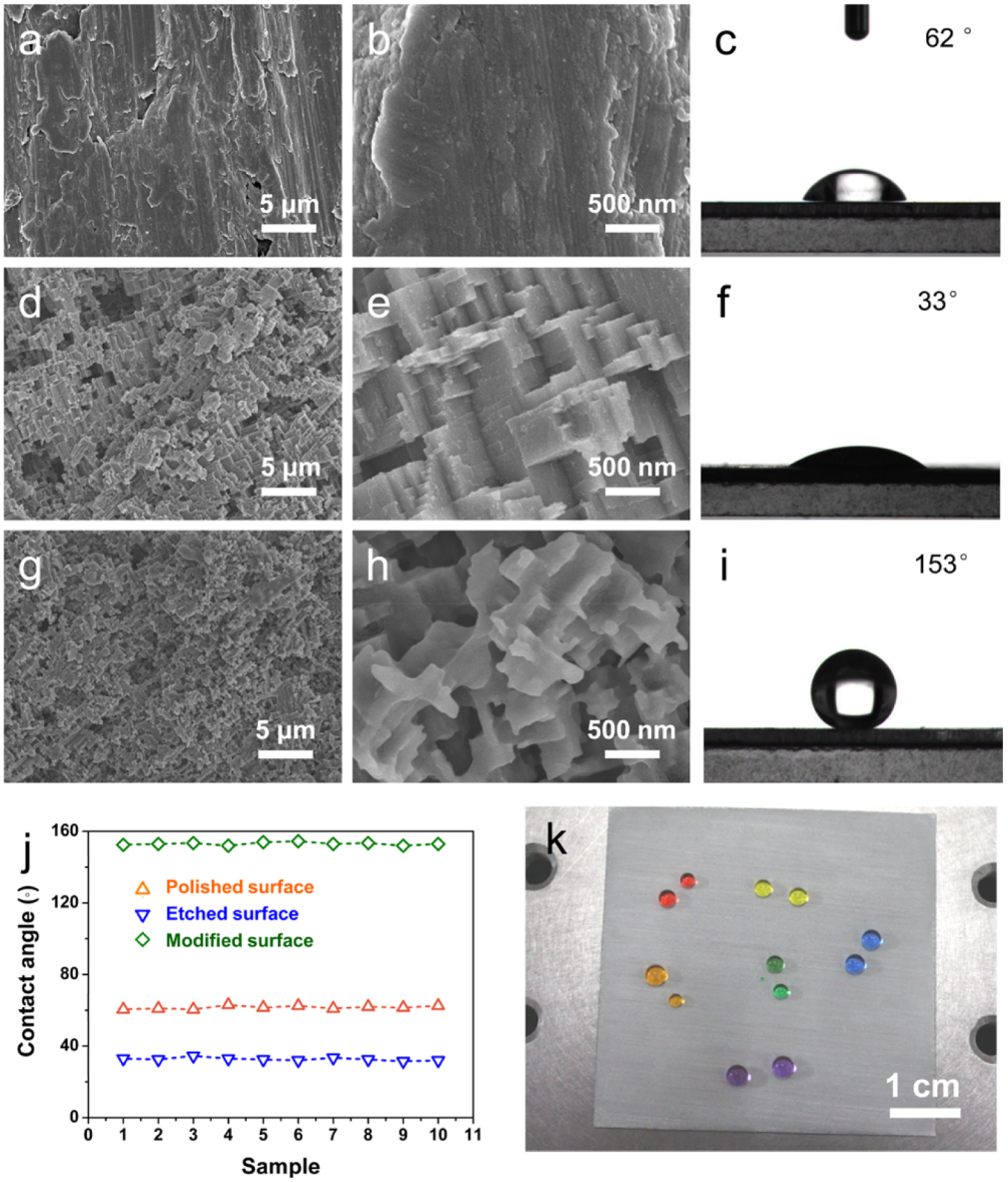

Figure 1. Superhydrophobic surfaces of the Al electrodes in the TENG. (a,b) SEM images of the polished Al electrodes with the low (a) and high (b) magnifications. (c) Measured contact angle of the polished Al electrode. (d,e) SEM images of the etched Al electrodes with the low (d) and high (e) magnifications. (f) Measured contact angle of the etched Al electrode. (g,h) SEM images of the modified Al electrodes with the low (g) and high (h) magnifications. (i) Measured contact angle of the modified Al electrode. (j) Measured contact angles of the different Al surfaces. (k) Photograph of the water drops on the superhydrophobic surface of the Al electrode.

TENG consists of a polyamide (PA) film as the wind-induced vibration layer and two Al electrodes covered by superhydrophobic films with a contact angle of about 153°. No output voltage/current decrease of the TENG can be observed after continuous working for about 14 h at a wind speed of 12 m/s. Through a power management circuit (PMC), the TENG can deliver a constant output voltage of 3.3 V and a pulsed output current of about 100 mA, which can charge a 10 mF capacitor to 2.7 V in 70 s, and the corresponding energy storage efficiency from the TENG into the capacitor by using the PMC has been enhanced by over 500 times as compared to using a rectifier. The fabricated TENG can be utilized to sustainably power a wireless smart temperature sensor node to send the real-time temperature data to an iPhone under a working distance of 26 m. This work can push forward a significant step toward wind energy scavenging and its potential applications in the self-powered wireless smart sensor networks.

RESULTS AND DISCUSSION

Figure 1a,b illustrates SEM images of the polished Al sheet, showing a smooth surface. The corresponding contact angle of the polished Al sheet is about 62°, as displayed in Figure 1c. The surface of the polished Al sheet was then chemically etched into nanostructures, as presented in Figure 1d,e, resulting in the corresponding contact angle decrease by about 33°, as illustrated in Figure 1f. Since the used Al sheet is a kind of hydrophilic material, the contact angle of the used Al sheet can be decreased when the Al sheet was etched into nanostructures on its surface. The etched surface of the polished Al sheet was then modified in 1.2 wt % 1H,1H,2H,2H-perfluorodecyltrichlorosilane/toluene solution, as diagramed in Figure 1g,h. The

DOI: 10.1021/acsnano.6b05815
ACS Nano 2016, 10, 9044−9052

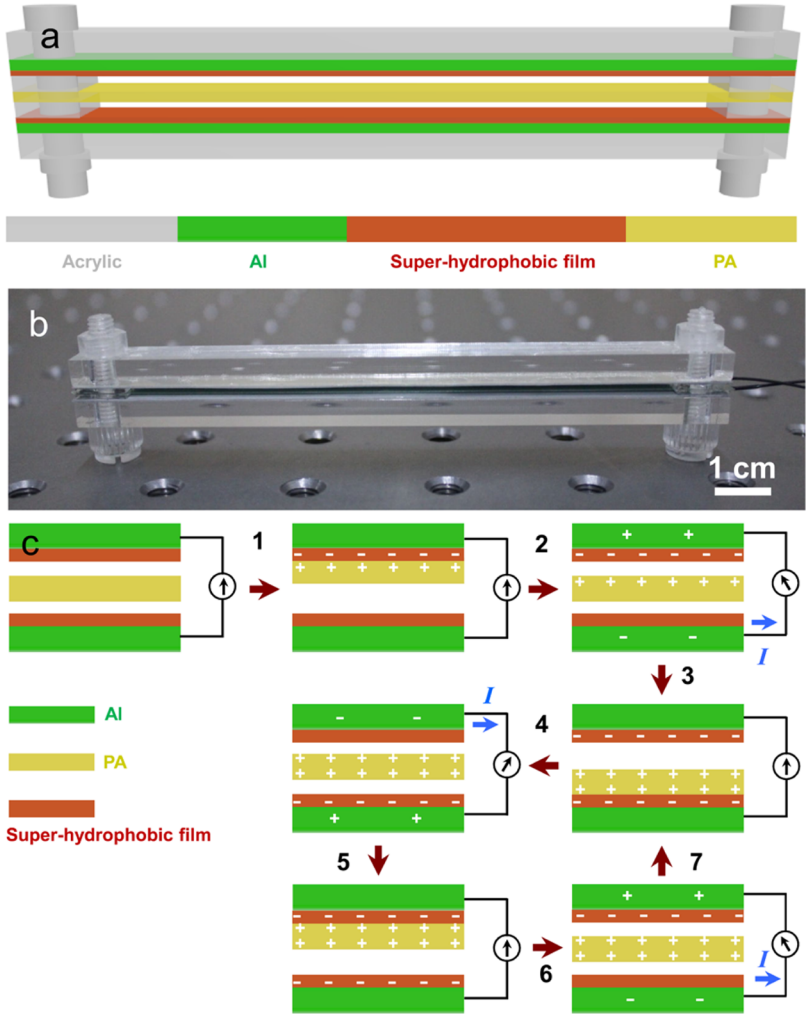

Figure 2. Device structure of the fabricated TENG and its operation principle. (a) Schematic diagram of the TENG. (b) Photograph of the TENG. (c) Schematic illustration of the operating principle for the TENG.

contact angle of the obtained superhydrophobic surface is about 153°, as displayed in Figure 1i. We measured the contact angles of 10 samples at the different surfaces, as shown in Figure 1j, confirming that the change in the contact angles under the different surfaces is similar as compared to that of the polished Al surface. Figure 1k illustrates a photograph of the superhydrophobic surface with several water drops on it, which can be also observed in movie file 1 (Supporting Information).

Figure 2a displays a schematic diagram of the fabricated TENG, which includes a PA at the middle of the device and two Al electrodes covered by two superhydrophobic films. As depicted in Figure 2b, the TENG has a dimension of 120 × 10 × 3 mm, where the distance of the air gap between the PA film and the top/bottom Al electrode is about 0.8 mm. Figure 2c illustrates the working mechanism of the TENG. First, when the PA film was at the middle of the device, there is no output current/voltage between the two Al electrodes. When the PA film was moved up to contact the top superhydrophobic film, the electrons can be injected from the PA film to the superhydrophobic film due to the different triboelectric polarities. There is also no output current/voltage between two Al electrodes in the process-1. When the PA film was moved down due to the wind-induced vibration, the electrons can flow from the top Al electrode to the bottom Al electrode due to electrostatic induction. When the PA film was moved down to contact the bottom of the superhydrophobic film, the electrons can be injected from the PA film into the bottom superhydrophobic film. After the process-3, the output current/voltage signals can be observed between the two Al electrodes when the PA film vibrated between the two superhydrophobic films.

As illustrated in Figure 3a,b, the TENG can generate an output voltage of about 218 V and an output current of about 30 μA at a wind speed of 12 m/s. Figure 3c depicts the measured output current peaks as a function of different external loading resistances ranging from 100 kΩ to 10 MΩ, showing the output current decreases with increasing the loading resistances. The corresponding largest output power of the TENG is about 2.2 mW under a loading resistance of 5 MΩ. For a new PA film without triboelectric charges on its surface, it can be seen that the output current of the TENG can be increased from 0 to 30 μA in about 100 s due to the triboeletric charging process, as displayed in Figure 3d. As illustrated in Figure 3e, both the output voltage and current can be increased with increasing the wind speeds, where the detailed data have been depicted in Supporting Information Figures S1 and S2. By calculating the time between two adjacent voltage peaks, the vibration frequency of the PA film can be found to increase with increasing the wind speeds (Figure 3f), where the corresponding working frequency of the

DOI: 10.1021/acsnano.6b05815
ACS Nano 2016, 10, 9044−9052

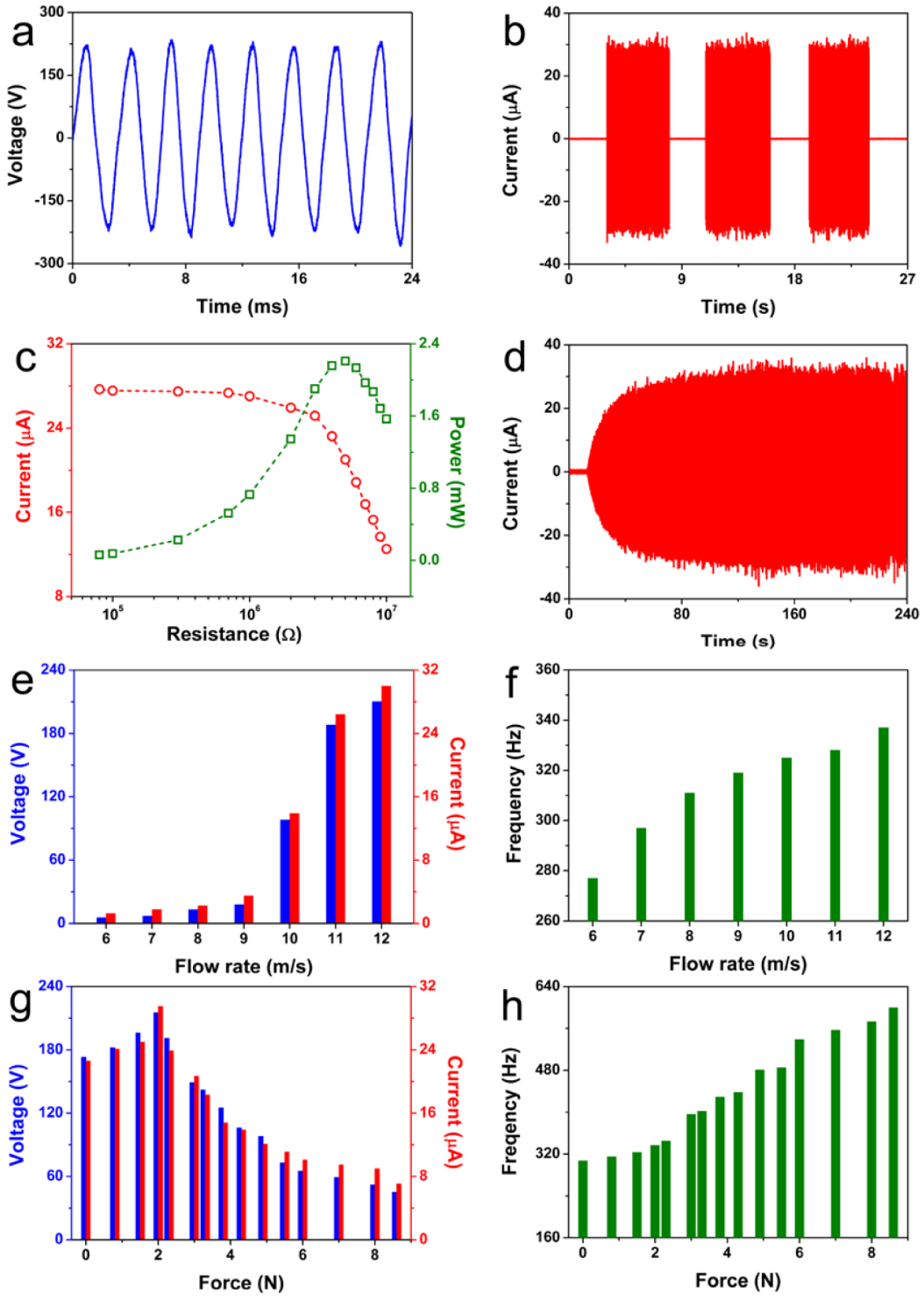

Figure 3. Output performance of the fabricated TENG related to different wind speeds and stretched forces. (a,b) Measured output voltage (a) and current (b) signals of the TENG. (c) Measured output current and calculated output power of the TENG under the different loading resistances. (d) Measured output current signals of a new TENG with increasing the time. (e,f) Measured output voltage/current (e) and the working frequency (f) of the TENG under the different wind speeds. (g,h) Measured output voltage/current (g) and the working frequency (h) of the TENG under the stretched forces.

TENG is about 337 Hz at a wind speed of 12 m/s. To understand the effect of the stretched forces applied in the PA film on the output performance of the TENG, the output voltage and current signals of the TENG were measured under the different stretched forces (Figure 3g), showing that both the output voltage and current of the TENG can be increased with increasing the stretched forces from 0 to 2 N and then can be decreased with increasing forces further from 2 to 8.6 N, where the detailed data have been displayed in Supporting Information Figures S3−S6. Under a stretched force of about 2 N, the TENG has the largest output voltage and current. Moreover, it can be found that the working frequency of the

DOI: 10.1021/acsnano.6b05815
ACS Nano 2016, 10, 9044−9052

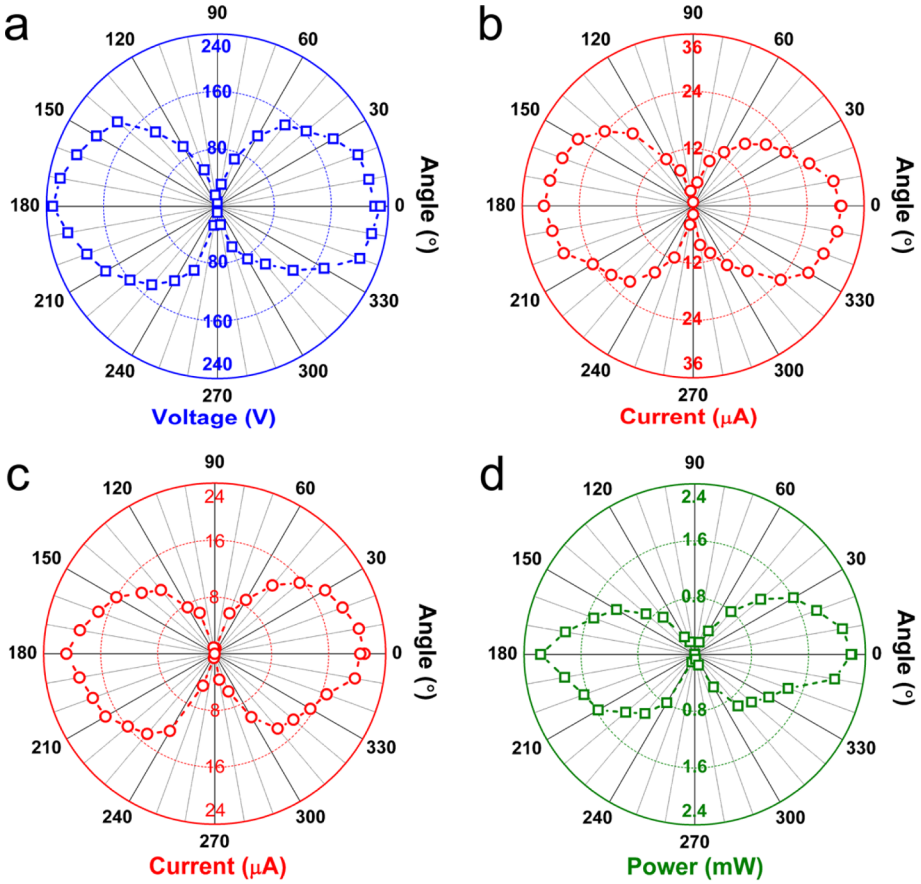

Figure 4. Output performances of the fabricated TENG under the different wind directions. (a,b) Measured output voltage (a) and current (b) signals of the TENG under the different wind directions ranged from 0° to 360°. (c,d) Under a loading resistance of 5 MΩ, measured output current signals (c) and the corresponding output powers (d) of the TENG under the different wind directions ranged from 0° to 360°.

TENG can be increased with increasing the applied forces on the PA film (Figure 3h), where the corresponding working frequency can be up to 600 Hz under a stretched force of about 8.6 N.

To understand the relationship between the output performances of TENG and the wind directions, we measured output voltage and current signals of the TENG under the different angles between the wind direction and the device width direction ranging from 0° to 360°. As illustrated in Figure 4a,b, both the output voltage and current signals can be decreased with increasing the angles. Under the angle of 90°, no output voltage or current signals can be observed. The output voltage and current of the TENG have the largest values at the angles of 0° or 180°. Figure 4c displays the output current signals of the TENG under a loading resistance of 5 MΩ at the different angles, exhibiting that the TENG can scavenge the wind energy from all directions. Moreover, Figure 4d depicts the corresponding output powers of the TENG under the different angles, exhibiting a similar change tendency for the output voltage and the output current. The output voltage and current stability of the TENG are displayed in Figure 5a, indicating that no decrease of the output voltage and current can be observed after the TENG was continuously working for 14 h. The ultrastable output performance of the TENG is important for the practical applications of the energy-harvesting devices. The good stability of the TENG is associated with the vibration film without metal electrodes on its surfaces.

To exploit the TENG as a power source of a wireless smart sensor node, the produced electricity from the TENG needs to be stored in a capacitor. The AC output voltage/current signals should be converted into DC output signals by utilizing a full wave bridge rectification circuit. As depicted in Supporting Information Figure S7, the rectified output voltage and current of the TENG are about 205 V and 28 μA, respectively. As compared with the output voltage/current in Figure 3a,b, there is a slight decrease due to the electricity consumption in the circuit. Figure 5b displays the charging curves of the different capacitors by using the TENG with a rectifier, showing that more charging time is needed for the larger capacitor, where the 1000 μF capacitor can be charged from 0 to 3 V in about 300 s of charging time. To increase the energy storage efficiency, it is necessary to decrease the output voltage of the TENG. As presented in Figure 5c, after using a transformer, the output voltage of the TENG can be decreased from 218 to 9.6 V. As a result, the output current of the TENG can be increased to 0.4 mA (Figure 5d). Although the output current of the TENG can be enhanced by using a transformer, the output current of the TENG after using a transformer still exhibit AC output characteristics. As illustrated in Figure 5e,f, the TENG after using a power management circuit (PMC) can deliver a DC output voltage of 3.3 V and a pulsed output current of 100 mA. To compare the charging performances of TENG with the different methods, a 10 mF capacitor was utilized as the storage unit. As displayed in Figure 5g, the TENG with a rectifier has a lowest charging performance as compared with the TENG with

DOI: 10.1021/acsnano.6b05815
ACS Nano 2016, 10, 9044−9052

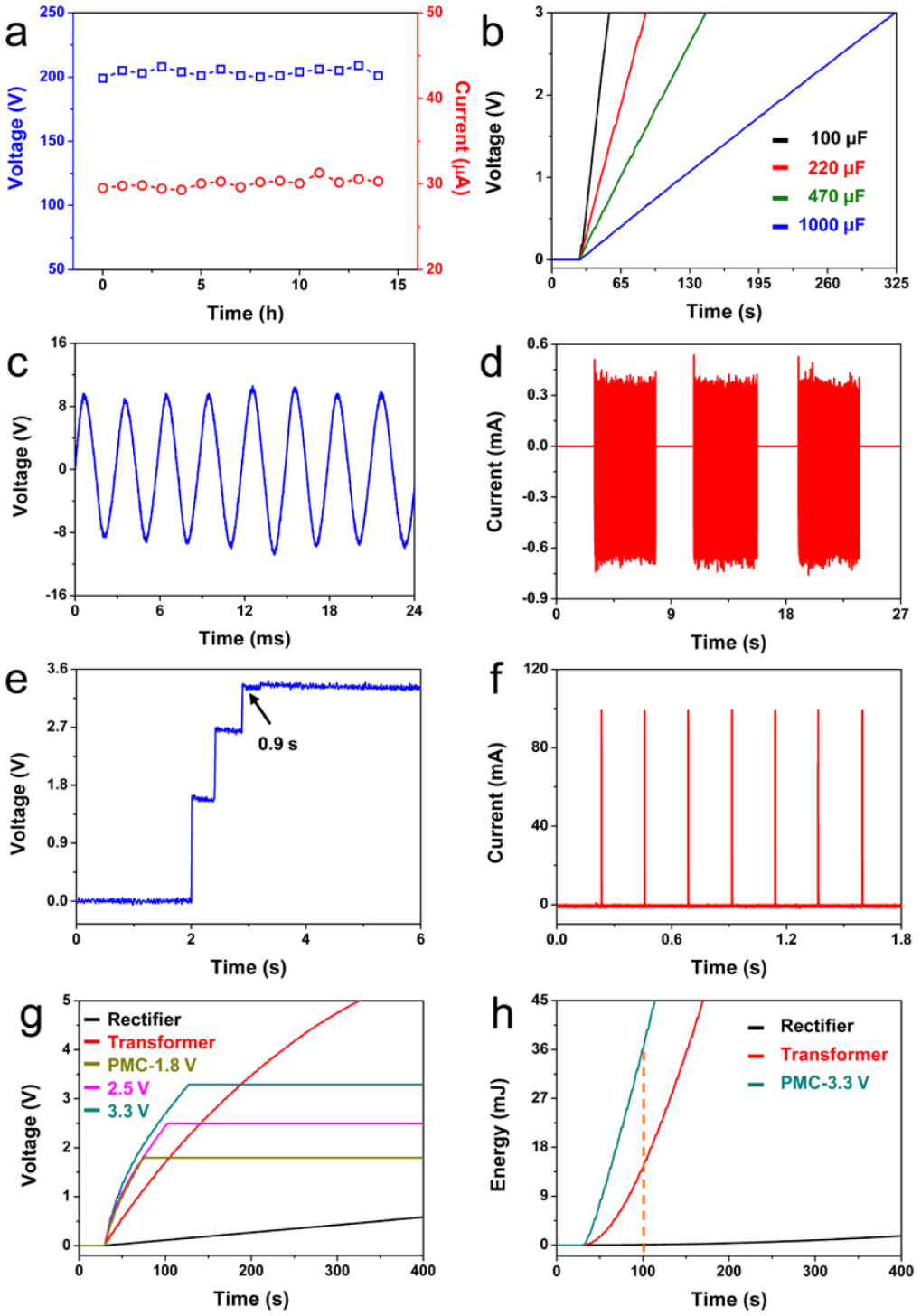

Figure 5. Stability, output performance, and charging performance of the TENG. (a) Stability measurement of the TENG. (b) Charging curves of the different capacitors by using the TENG with a rectifier. (c,d) Measured output voltage (c) and current (d) signals of the TENG after using a transformer. (e,f) Measured output voltage (e) and current (f) signals of the TENG after using a PMC. (g) Measured charging curves of a 10 mF capacitor by using the TENG with different methods. (h) The stored energy in the 10 mF capacitor by using the TENG with different methods.

a transformer or a PMC. The TENG with a PMC has the best charging performance among the three methods. By using the different PMCs, the output voltage can modulated such as 1.8 or 2.5 V, where the corresponding output voltage and current signals of the TENG are as displayed in Supporting Information Figure S8. Moreover, it can be seen that the voltage of the capacitor can be kept at a fixed value by using a PMC, which is important for protecting the safety of connecting the wireless smart sensor node. If a transformer was used to power the wireless smart sensor, the continuous increase of the charging voltage can result in the failure or breakdown of the sensor. Figure 5h illustrates the stored energy in the 10 mF capacitor by using the TENG with the different methods. After the capacitor was charged in 70 s, the stored

DOI: 10.1021/acsnano.6b05815
ACS Nano 2016, 10, 9044−9052

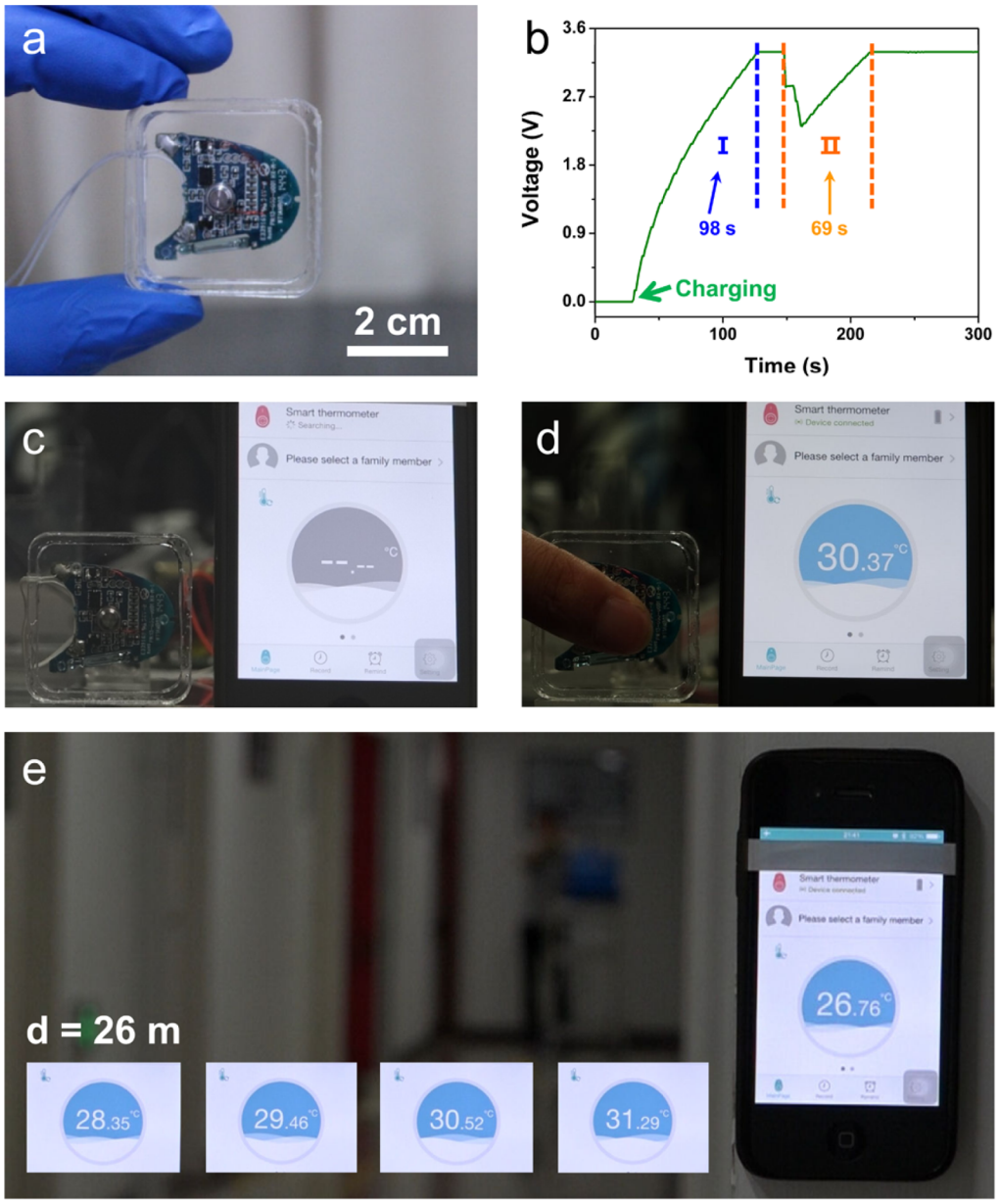

Figure 6. Self-powered wireless smart temperature sensor node. (a) Photographs of the used wireless smart temperature sensor. (b) Charging curve of a 10 mF capacitor by using the TENG with a PMC to power the wireless smart temperature sensor. (c,d) Photographs of the wireless smart temperature sensor before (c) and after (d) being powered by the TENG. (e) Photograph of the wireless smart temperature sensor that can sustainably work by using the TENG to obtain the electric energy under a distance of 26 m.

energies by using the TENG with a rectifier, a transformer, and a PMC are 0.064, 14.35, and 35.96 mJ, respectively. The energy storage efficiency can be calculated using the ratio between the stored energy and the produced energy by the TENG in 70 s. As compared with the rectifier, the energy storage efficiency by using a transformer and a PMC can be enhanced by over 200 times and over 500 times, respectively.

To demonstrate a self-powered wireless smart sensor node, we fabricated a self-powered system including a TENG, a PMC, a 10 mF capacitor, a wireless smart temperature sensor node, and an iPhone for receiving the temperature data. Figure 6a displays a photograph of a wireless smart temperature sensor with a size of 4 × 4 × 0.7 cm. As presented in Figure 6b, the 10 mF capacitor can be charged from 0 to 3.3 V in 98 s in the process-1. When the wireless smart temperature sensor was turned on, the voltage of the capacitor was found to drop first and then increase to 3.3 V. The decrease in the capacitor voltage is due to fact that the produced electricity energy by the TENG is smaller than the energy consumption for the connection between the wireless sensor and the iPhone. When the wireless sensor was connected to the iPhone, the energy consumption for sending temperature data to the iPhone is smaller than the produced energy by the TENG, resulting in the increase of the capacitor voltage. After that, the wireless smart temperature sensor node can work all the time and send the temperature data to the iPhone. As shown in Figure 6c, no temperature data can be observed on the screen of the iPhone when the TENG was not working. When the TENG was working, the wireless smart temperature sensor can work and send the temperature data of a human finger touching the iPhone, showing a value of 30.37 °C (Figure 6d), which can be also seen in movie file 2 (Supporting Information). The self-

DOI: 10.1021/acsnano.6b05815
ACS Nano 2016, 10, 9044−9052

powered wireless smart temperature sensor node can sustainably work and send the temperature data to the iPhone under a distance of 26 m, as illustrated in Figure 6e and movie file 3 (Supporting Information).

A self-powered wireless smart temperature sensor node has been achieved by using the TENG to scavenge wind energy as the power source instead of using a Li-ion battery. As compared with previous TENGs, the fabricated TENG has the following three advantages: First, the TENG has the superhydrophobic surfaces with a contact angle of about 153°, which is important for realizing the self-cleaning function and the sustainable working of the TENG without the effect of external weather. Second, most of the previous TENGs cannot endure the continuous working for a long time due to the damage of the metal electrode on the triboelectric film. In this study, an ultrastable output performance of the TENG has been achieved, where there is no decrease for the output voltage and current of the TENG after continuous working of about 14 h at a wind speed of 12 m/s. The ultrastable output performance is associated with not using the metal electrode on the triboelectric vibration film. The obtained ultrastable output performance of the TENG is important for pushing the practical applications of this device. Third, the working of most commercial sensors requires a low voltage (<5 V) and a high current (>1 mA). However, most of previous TENGs have the high output voltage (>100 V) and a low output current (<100 μA). In this study, a low output voltage and a high output current of the TENG have been realized by using a PMC, where the TENG with the PMC can deliver a constant output voltage of 3.3 V and a pulsed output current of about 100 mA. The optimized output performance of the TENG is important for directly powering some commercial devices.

In addition, the energy storage efficiency from the TENG to the capacitor has been dramatically enhanced. Most of the TENGs were utilized to charge a capacitor by using a rectifier. However, we found that charging a capacitor by using the TENG with a PMC or a transformer will be much better than by using a rectifier. In this study, after a 10 mF capacitor was charged in 70 s, the stored energies by using the TENG with a rectifier, a transformer, and a PMC are 0.064, 14.35, and 35.96 mJ, respectively. As compared with the rectifier, the energy storage efficiency by using a PMC can be enhanced by over 500 times. For the practical application of the TENG, we have achieved a total system including a TENG, a PMC, a 10 mF capacitor, a wireless smart temperature sensor node, and an iPhone for receiving the temperature data. The self-powered wireless smart temperature sensor node can sustainably work well and send the temperature data to an iPhone under a distance of 26 m. This TENG can also be used as the power source for providing electricity to the other wireless smart sensors nodes. Future work can involve further improvements of the output performance of TENG and the hybridization of the different energies to realize the maximizing output of the energy harvester for the self-powered wireless smart sensor networks.

CONCLUSIONS

In summary, we have rationally designed an ultrastable, highly efficient, and superhydrophobic-surface-based TENG to scavenge wind energy from all directions for sustainably powering a wireless smart temperature sensor node. There is no decrease for the output voltage and current of the TENG after continuous working for about 14 h at a wind speed of 12 m/s. Through a PMC, the TENG can deliver a constant output voltage of 3.3 V and a pulsed output current of about 100 mA, where the energy storage efficiency from the TENG into a 10 mF capacitor by using the PMC can be enhanced by over 500 times as compared with that by using a rectifier. A wireless smart temperature sensor node can be sustainably powered by the TENG for sending the real-time temperature data to an iPhone under a working distance of 26 m, demonstrating the feasibility of the self-powered wireless smart sensor networks.

METHODS

Preparation of Superhydrophobic Surfaces in the TENG. Aluminum sheets were polished and ultrasonically cleaned in alcohol and washed with deionized water. After this, they were then chemically etched by immersion in a mixed solution (36% HCl and H_2O with volume ratio in 1:15) in plastic beakers at room temperature for 1 min. After etching, the aluminum sheets were immediately rinsed ultrasonically with deionized water and washed with ethanol, followed by drying, and then placed in an oven at 120 °C for 5 min. The etched aluminum sheets were modified in 1.2 wt % 1H,1H,2H,2H-perfluorodecyltrichlorosilane/toluene solution at room temperature for 10 h. After removal from the solution, the substrates were heat treated at 140 °C for 2 h. A PA film (120 × 10 × 0.05 mm) was ultrasonically cleaned in alcohol, washed with water, and then dried at room temperature. After drying, the PA film was immersed in the hydrophobic solution (Zixilai Technology, China) for 10 min at room temperature. After removal from the solution, the PA film dried at room temperature for 12 h.

Fabrication of the TENG. The fabricated TENG consists of a PA film and two aluminum electrodes covered with the superhydrophobic films. The working of TENG is based on the wind-induced vibration of the PA film to realize the periodic contact and separation between two different triboelectric materials. Two acrylic plates (120 × 10 × 5 mm) as the substrates were cut by using a laser cutting machine. Two holes with a diameter of 5 mm were fabricated at both ends of the acrylic sheets. The supporting beams (10 × 10 × 0.8 mm) were fixed between two acrylic sheets. Screws were used to fix the two ends of the PA film in the middle of the TENG. When the wind flowed into the device, the PA film can vibrate up and down to contact the aluminum sheets with the superhydrophobic films, resulting in the observed output voltage/current signals.

Measurement of the Fabricated Device. Contact angles were measured with an optical contact angle meter at room temperature. Water droplets were dropped onto the surfaces, and the average value of 10 measurements at different positions of the sample was adopted as the contact angle. The stretched forces of the PA film were measured with a digital tensometer. The morphology of the aluminum sheets with the polished, etched, and modified surfaces was performed using a field-emission scanning electron microscope (SU8020). The output voltage and current signals of the TENG were obtained by using a mixed domain oscilloscope (Tektronix MDO3024) and a low-noise current preamplifier (Stanford Research SR570), respectively.

ASSOCIATED CONTENT

Supporting Information

The Supporting Information is available free of charge on the ACS Publications website at DOI: 10.1021/acsnano.6b05815.

Additional figures include measured output voltage and current signals of the TENG under different wind speeds and under different stretched forces by using a rectifier and by using two different PMCs (PDF)

Water drops of different colors on the surface of the superhydrophobic film (AVI)

A wireless smart temperature sensor powered by the TENG (AVI)

DOI: 10.1021/acsnano.6b05815
ACS Nano 2016, 10, 9044−9052

A wireless smart temperature sensor driven by the TENG to send the temperature data to an iPhone under the different distances ranged from 0 m to 26 m (3 times of the normal speed) (AVI)

AUTHOR INFORMATION

Corresponding Author

*E-mail: yayang@binn.cas.cn.

Notes

The authors declare no competing financial interest.

ACKNOWLEDGMENTS

This work was supported by Beijing Natural Science Foundation (2154059), the National Natural Science Foundation of China (grant nos. 51472055 and 61404034), External Cooperation Program of BIC, Chinese Academy of Sciences (grant no. 121411KYS820150028), the 2015 Annual Beijing Talents Fund (grant no. 2015000021223ZK32), the National Key R & D Project from Minister of Science and Technology in China (grant no. 2016YFA0202701), and the "thousands talents" program for the pioneer researcher and his innovation team, China. The corresponding patent has been submitted based on this work presented here.

REFERENCES

(1) Xu, S.; Zhang, Y.; Jia, L.; Mathewson, K. E.; Jang, K.-I.; Kim, J.; Fu, H.; Huang, X.; Chava, P.; Wang, R.; Bhole, S.; Wang, L.; Na, Y. J.; Guan, Y.; Flavin, M.; Han, Z.; Huang, Y.; Rogers, J. A. Soft Microfluidic Assemblies of Sensors, Circuits, and Radios for the Skin. *Science* **2014**, *344*, 70−74.

(2) Jeon, J.; Lee, H.-B.-R.; Bao, Z. Flexible Wireless Temperature Sensors based on Ni Micropaticale-Filled Binary Polymer Composites. *Adv. Mater.* **2013**, *25*, 850−855.

(3) Huang, X.; Liu, Y.; Chen, K.; Shin, W.-J.; Lu, C.-J.; Kong, G.-W.; Patnaik, D.; Lee, S.-H.; Cortes, J. F. J.; Rogers, A. Stretchable, Wireless Sensors and Functional Substrates for Epidermal Charaterization of Sweat. *Small* **2014**, *10*, 3083−3090.

(4) Kang, B.; Ceder, G. Battery Materials for Ultra Fast Charging and Discharging. *Nature* **2009**, *458*, 190−193.

(5) Kovalenko, I.; Zdyrko, B.; Magasinski, A.; Hertzberg, B.; Milicev, Z.; Burtovyy, R.; Luzinov, I.; Yushin, G. A Major Constituent of Brown Algae for Use in High-Capacity Li-ion Batteries. *Science* **2011**, *334*, 75−79.

(6) Dunn, B.; Kamath, H.; Tarascon, J.-M. Electrical Energy Storage for the Grid: a Battery of Choices. *Science* **2011**, *334*, 928−935.

(7) Wu, Y.; Wang, X.; Yang, Y.; Wang, Z. L. Hybrid Energy Cell for Harvesting Mechanical Energy from One Motion Using Two Approaches. *Nano Energy* **2015**, *11*, 162−170.

(8) Quan, T.; Wang, X.; Wang, Z. L.; Yang, Y. Hybridized Electromagnetic-Triboelectric Nanogenerator for a Self-Powered Electrnic Watch. *ACS Nano* **2015**, *9*, 12301−12310.

(9) Chun, J.; Kim, J. W.; Jung, W.; Kang, C.-Y.; Kim, S.-W.; Wang, Z. L.; Baik, J. M. Mesoporous Papers Impreganted with Au Nanoparticles as Effective Dielectrics for Enhancing Triboelectric Nanogenerator Performance in Harsh Environments. *Energy Environ. Sci.* **2015**, *8*, 3006−3012.

(10) Chung, J.; Lee, S.; Yong, H.; Moon, H.; Choi, D.; Lee, S. Self-Packing Elastic Bellows-Type Triboelectric Nanogenerator. *Nano Energy* **2016**, *20*, 84−93.

(11) Lee, J.-H.; Hinchet, R.; Kim, T. Y.; Ryu, H.; Seung, W.; Yoon, H.-J.; Kim, S.-W. Control of Skin Potential by Triboelectrification with Ferroelectric Polymers. *Adv. Mater.* **2015**, *27*, 5553−5558.

(12) Kim, K. N.; Jung, Y. K.; Chun, J.; Ye, B. U.; Gu, M.; Seo, E.; Kim, S.; Kim, S.-W.; Kim, B.-S.; Baik, J. M. Surface Dipole Enhanced Instantaneous Charge Pair Generation in Triboelectric Nanogenerator. *Nano Energy* **2016**, *26*, 360−370.

(13) Guo, H.; Leng, Q.; He, X.; Wang, M.; Chen, J.; Hu, C.; Xi, Y. A Triboelectric Generator Based on Checker-Like Interdigital Electrodes with a Sandwiched PET Thin Film for Harvesting Sliding Energy in All Directions. *Adv. Energy Mater.* **2015**, *5*, 1400790.

(14) Zhong, X.; Yang, Y.; Wang, X.; Wang, Z. L. Rotating-Disk-Based Hybridized Electromagentic-Triboelectric Nanogenerator for Scavenging Biomechanical Energy as a Mobile Power Source. *Nano Energy* **2015**, *13*, 771−780.

(15) Guo, H.; Chen, J.; Tian, L.; Leng, Q.; Xi, Y.; Hu, C. Airflow-Induced Triboelectric Nanogenerator as a Self-Powered Sensor for Detecting Humidity and Airflow Rate. *ACS Appl. Mater. Interfaces* **2014**, *6*, 17184−17189.

(16) Bae, J.; Lee, J.; Kim, S.; Ha, J.; Lee, B.-S.; Park, Y.; Choong, C.; Kim, J.-B.; Wang, Z. L.; Kim, H.-Y.; Park, J.-J.; Chung, U.-I. Flutter-Driven Triboelectrification for Harvesting Wind Energy. *Nat. Commun.* **2014**, *5*, 4929.

(17) Guo, H.; He, X.; Zhong, J.; Zhong, Q.; Leng, Q.; Hu, C.; Chen, J.; Tian, L.; Xi, Y.; Zhou, J. A Nanogenerator for Harvesting Airflow Energy and Light Energy. *J. Mater. Chem. A* **2014**, *2*, 2079−2087.

DOI: 10.1021/acsnano.6b05815
ACS Nano 2016, 10, 9044−9052